Colloidal mesoporous silica nanoparticles with protoporphyrin IX encapsulated for photodynamic therapy

Jun Qian
Arash Gharibi
Sailing He
Zhejiang University
Joint Research Center of Photonics of the Royal Institute of Technology (Sweden)
and
Zhejiang University
Centre for Optical and Electromagnetic Research
Zijingang Campus, Hangzhou 310058
China

Abstract. Protoporphyrin IX (PpIX)-encapsulated mesoporous silica nanoparticles were synthesized, characterized, and utilized for photodynamic therapy (PDT) of cancer. Silica encapsulation is relatively transparent for activated light and can protect the PpIX against denaturation induced by the extreme bioenvironment. The mesoporous silica can also ensure that the encapsulated PpIX can be well-contacted with oxygen, stimulated, and released. PpIX-encapsulated colloidal mesoporous silica nanoparticles were uptaken by tumor cells *in vitro*, and the effect of photon-induced toxicity was demonstrated after comparison with some control experiments. The surface of PpIX-encapsulated silica nanoparticles can be grafted with appropriate functionalized groups and conjugated with certain biomolecules for specific targeting. [DOI: 10.1117/1.3083427]

Keywords: PpIX-encapsulated silica nanoparticles; fluorescence imaging; uptake; photodynamic therapy.

Paper 08266R received Aug. 4, 2008; revised manuscript received Nov. 17, 2008; accepted for publication Dec. 4, 2008; published online Feb. 27, 2009.

1 Introduction

Photodynamic therapy (PDT) is a light-activated treatment for malignant or premalignant cancer tumors and other diseases. It has emerged as an important research area in biophotonics.[1–4] PDT is based on the fact that some photosensitizers (PSs) can be accumulated to a higher concentration in tumor cells than in healthy cells upon systemic administration. By matching the wavelength of the therapeutic light to the absorption peak of the sensitizers, most of the light is absorbed by the PSs, and the excited PS molecules can then transfer their energy to surrounding oxygen molecules, which are normally in their triplet ground state. This results in the formation of reactive oxygen species (ROSs) such as singlet oxygen ($^1O_2$) or free radicals. ROSs are responsible for oxidizing various cellular compartments, resulting in irreversible damage to tumor cells.[2–4] PSs, oxygen, and light are three crucial components for this photon-induced toxicity effect.[5,6]

Most existing PSs are hydrophobic and may aggregate easily in a biological environment.[7,8] Even for hydrophilic PSs, the selective accumulation in tumor tissues is not high enough for clinical use. To overcome these limitations, colloidal carriers for PSs, such as liposomes and polymeric micelles, have been investigated.[9,10] For the study described in this paper, colloidal mesoporous silica nanoparticles with encapsulated protoporphyrin IX (PpIX), which has been widely investigated and officially approved for use in clinical treatments,[11,12] were synthesized and utilized as drug carriers. This nanoformulation has many advantages over PS-encapsulated polymer/liposomes. The PS-encapsulated silica nanoparticles can be easily prepared with a desired size, shape, and porosity, and are very stable.[13] They are more biocompatible than other nanomaterials, and they can effectively protect the doped PSs against denaturation induced by the extreme bioenvironment.[14] Silica encapsulation is relatively transparent for both the activated light and signal light. The mesoporosity property can also ensure oxygen contact with encapsulated PSs so that they can be effectively stimulated and released. The ultrasmall size ($<$50 nm) and surface charge of silica nanoparticles can help them be uptaken by tumor cells through the "enhanced permeability and retention effect,"[15,16] To accumulate PSs selectively in tumor tissues and reduce the dosage of PSs, their surfaces can be functionalized with various groups and further conjugated with antibodies for specific uptake in an *in vivo* experiment.[17]

In this paper, we report an investigation that used mesoporous silica nanoparticles with encapsulated PpIX for PDT treatment. The nanoparticles were synthesized, characterized, and utilized for *in vitro* imaging of tumor cells. The effect of photon-induced toxicity of this nanoformulation was also demonstrated after comparison with some control experiments. The PpIX-encapsulated mesoporous silica nanoparticles showed good potential applications to, e.g., photodynamic therapy for cancers.

Address all correspondence to: Sailing He, Joint Research Center of Photonics of the Royal Institute of Technology (Sweden) and Zhejiang University, Hangzhou, China. Tel: +86-571-88206525; Fax: +86-571-88206512; E-mail: sailing@kth.se.

1083-3668/2009/14(1)/014012/6/$25.00 © 2009 SPIE

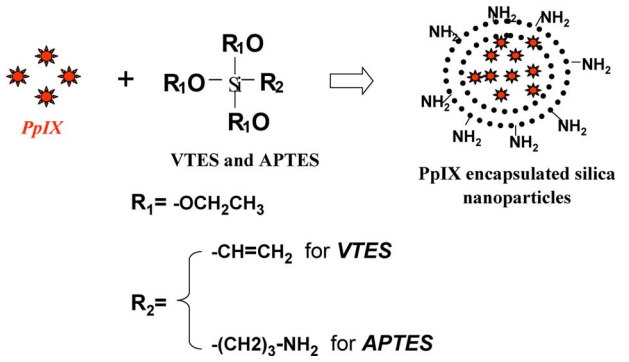

Fig. 1 Representative schematic showing the synthesis of PpIX-encapsulated silica nanoparticles. (Color online only.)

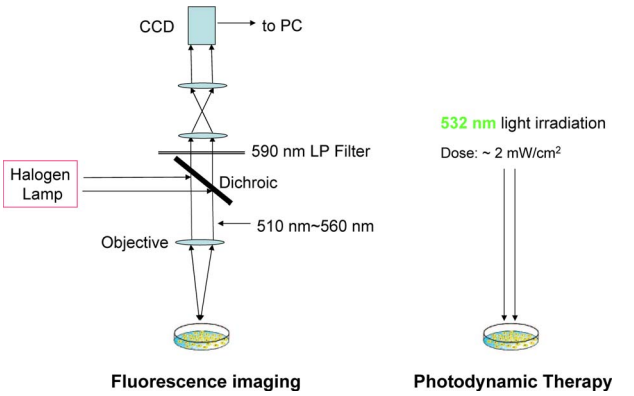

Fig. 2 Schematic illustration of the setup for fluorescence imaging and *in vitro* PDT of cells. (Color online only.)

2 Experiments

2.1 *Chemicals*

Aerosol-OT (98%), Vinyltriethoxysilane (VTES) (97%), (3-Aminopropyl)triethoxysilane (APTES) (98%), PpIX, and 1,3-diphenylisobenzofuran (DPBF) were purchased from Sigma Aldrich. Dimethylsulfoxide (DMSO) and 1-butanol (99.8%) were purchased from Sinopharm Chemical Reagent Co., Ltd. (China). Cell-culture products, unless otherwise mentioned, were purchased from GIBCO. All the above chemicals were used without any additional purification, and distilled (DI) water was used in all the experimental steps.

2.2 *Synthesis of PpIX-Encapsulated Silica Nanoparticles*

PpIX-encapsulated silica nanoparticles were synthesized in the nonpolar core of aerosol-OT/DMSO/ water micelles (as shown in Fig. 1).[13] Typically, the micelles were prepared by dissolving a certain amount of aerosol-OT and 1-butanol in 10 ml of DI water by vigorous magnetic stirring. PpIX in DMSO (10 mM) was then added to the solution under magnetic stirring. Half an hour later, a certain amount of neat VTES was added to the micellar system, and the resulting solution was stirred for about 1 hour. Next, silica nanoparticles were precipitated by adding APTES and stirred for 20 hours at room temperature. After the formation of the nanoparticles, surfactant aerosol-OT, cosurfactant 1-butanol, residual VTES, and APTES, and an extremely tiny amount of soluble PpIX molecules were removed by dialysis. The dialyzed solution was then filtered through a hydrophilic membrane filter with 0.45-μm cutoff to separate the PpIX-encapsulated silica nanoparticles from the PpIX. The PpIX molecules were barely soluble in DI water and their insoluble aggregates were blocked by the membrane, while the small hydrophilic silica nanoparticles could pass through the membrane very easily. The sample was kept for later use after purification. The same protocol was used to synthesize Nile red-encapsulated silica nanoparticles, which were used in some control experiments.

2.3 *Experimental Characterization*

Transmission electron microscope (TEM) analyses were made with JEOL's JEM-1200EX equipment. The as-synthesized PpIX-encapsulated silica nanoparticles were used for investigation. The ultraviolet (UV) and visible (vis) extinction spectra were recorded from 250 to 900 nm with a Shimadzu 2550 UV-vis scanning spectrophotometer at room temperature. The photoluminescence spectra were obtained by a fluorescence spectrophotometer (F-2500, HITACHI, Japan) with a xenon lamp excitation ranging from 180 to 800 nm.

2.4 *Detection of Reactive Oxygen Species (ROSs)*

Chemical oxidation of DPBF in the aqueous solution of the PpIX-encapsulated silica nanoparticles was used as an indirect method to characterize singlet oxygen generation efficiency.[18] In this case, the decrease in the absorbance of the DPBF added to the aqueous solution of the PpIX-encapsulated nanoparticles was monitored as a function of time after irradiation with 532-nm laser light.

2.5 *Cell Culture*

HeLa cells (human cancer cell lines) were cultivated in Dulbecco minimum essential media (DMEM) with 10% fetal bovine serum (FBS), 1% penicillin, and 1% amphotericin B. One day before the treatment, cells were seeded in 35-mm cultivation dishes at a confluence of 70 to 80%. During the treatment, a 200-μl stock solution of PpIX-encapsulated silica nanoparticles was added to a HeLa cell plate. A 200-μl stock solution of Nile red-encapsulated silica nanoparticles was added to another HeLa cell plate for a control experiment. A third HeLa cell plate without any treatment was used for another control experiment. The cell incubation process lasted for 2 hours at 37 °C with 5% CO_2. Then the cells were washed thrice with phosphate buffered saline (PBS) and directly imaged using a microscopy.

2.6 *Fluorescence Imaging*

Fluorescence imaging of cells was taken from a Nikon E200 microscope (as shown in Fig. 2). Green light (510 to 560 nm, with a maximal spectrum peak at 535 nm) was used to excite the cell sample through the same 40×/0.65 objective lens that collected the fluorescence signal for imaging. After passing through a long wavelength-pass (LP) optical filter (590-nm LP), all the fluorescence signals were received by the CCD, which was installed on the top of the microscope, and then transferred to software in a personal computer.

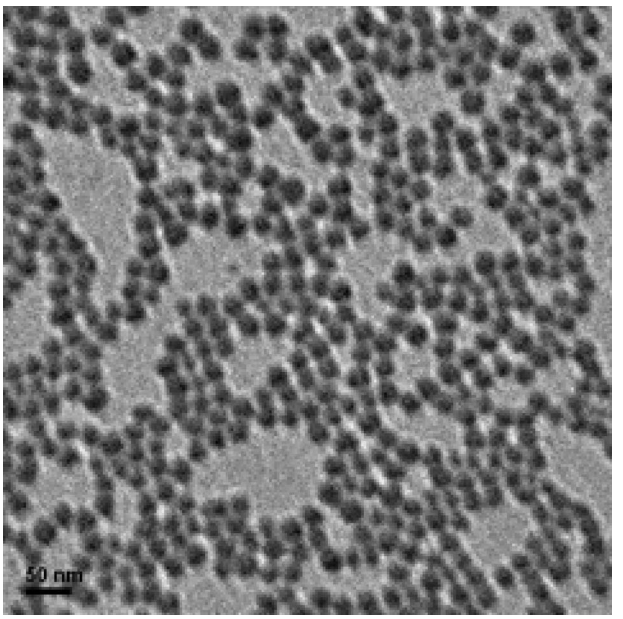

Fig. 3 TEM image of some PpIX-encapsulated silica nanoparticles (scale bar is 50 nm).

2.7 *In Vitro PDT*

To confirm the photon-induced toxicity effect of PpIX-encapsulated silica nanoparticles, HeLa cells targeted by them were irritated by a 532-nm light source at the dosage of $\sim 2\ \mathrm{mW/cm^2}$ for 2 minutes (as shown in Fig. 2). Cells were observed and imaged under the microscope. Over the next 8 minutes, cell images were successively recorded every 2 minutes for further analysis. In the control experiments, the same experimental procedure was also carried out for HeLa cells targeted by the Nile red-encapsulated nanoparticles and the nontreated HeLa cells.

3 Results and Discussion

3.1 *Characterization of PpIX-Encapsulated Silica Nanoparticles*

Figure 3 is the TEM image of the PpIX-encapsulated silica nanoparticles. These nanoparticles were all spherical in shape, highly monodispersed, and had an average diameter of 25 nm.

The extinction spectra and fluorescence emission spectra of PpIX before (in DMSO) and after encapsulation (in water) are shown in Fig. 4. The extinction spectra of the aqueous solution of PpIX-encapsulated nanoparticles were similar to the extinction spectra of the PpIX in DMSO solution around their spectra peaks (about 405 nm; these extinction peaks are mainly due to the absorption). However, the PpIX-encapsulated silica nanoparticles extincted more light than the PpIX in DMSO. The difference mainly arose from the Rayleigh scattering by the nanoparticles, since the nanoparticles were about 25 nm in diameter (comparable to light wavelengths) while PpIX molecules were only about 1 nm in diameter and their scattering effect was almost negligible. According to Mie theory,[19,20] the scattering and absorption efficiencies are given by

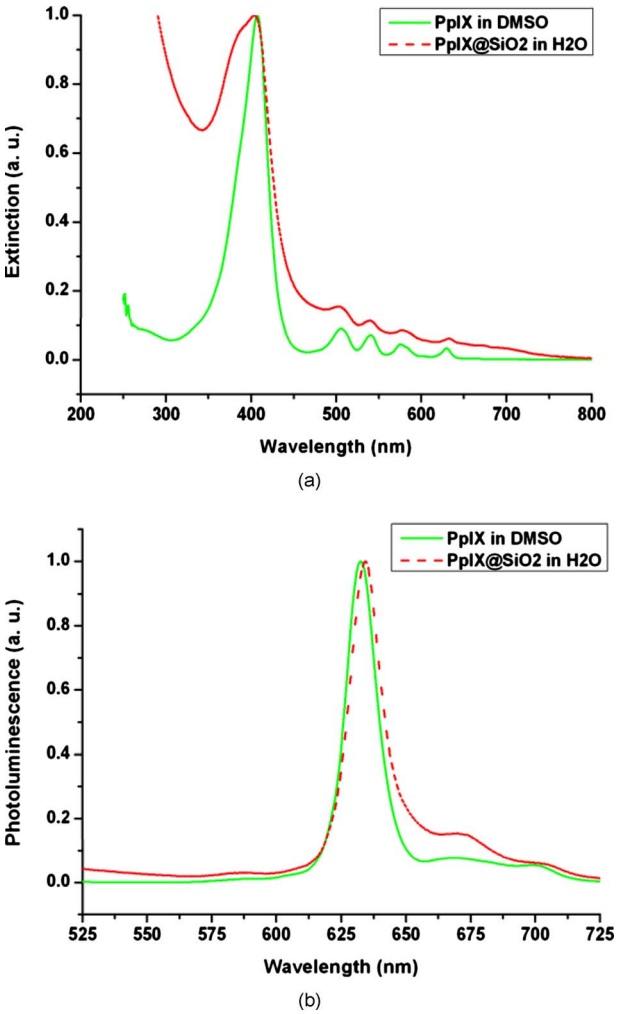

Fig. 4 (a) Extinction and (b) fluorescence emission spectra of PpIX before (in DMSO) and after being encapsulated (in water) by silica nanoparticles. (Color online only.)

$$Q_{sca} = \frac{8}{3}\pi^4 n_m^4 \left(\frac{d}{\lambda}\right)^4 \left|\frac{m^2-1}{m^2+2}\right|^2 \text{ and } Q_{abs} = \frac{4\pi n_m d}{\lambda}\,\mathrm{Im}\left\{\frac{m^2-1}{m^2+2}\right\}\left[1+\frac{4}{3}\left(\frac{\pi n_m d}{\lambda}\right)^4 \mathrm{Im}\left\{\frac{m^2-1}{m^2+2}\right\}\right],$$

respectively, where d is the diameter of the silica nanoparticle or PpIX molecule, λ is the wavelength, n_m is the refractive index of the medium, and m is a relative refractive index (complex) defined by $m(\lambda)=n/n_m$ (n is the refractive index of the silica nanoparticles or PpIX molecules). For PpIX molecules, the average diameter was only about 1 nm; thus, the factor $\frac{8}{3}\pi^4 n_m^4 (d/\lambda)^4$ was very small and negligible. Since $m(\lambda)=(n_{\mathrm{PpIX}}+i^* n'_{\mathrm{PpIX}})/n_m$ (where n'_{PpIX} is related with the absorption of PpIX molecules), the factor $|m^2-1/m^2+2|^2$ could not be very large unless $n_{\mathrm{PpIX}}/n_m \to 0$ (not true) and $n'_{\mathrm{PpIX}}/n_m \to \pm\sqrt{2}$. Therefore, the scattering efficiency for the DMSO solution of PpIX molecules was negligible. For silica nanoparticles, the average diameter was about 25 nm (much larger than the average diameter for the PpIX molecules), and thus the factor $\frac{8}{3}\pi^4 n_m^4 (d/\lambda)^4$ was not negligible. The factor

$|m^2-1/m^2+2|^2$ was not negligible, either (otherwise, Im$\{m^2-1/m^2+2\}$ should be very small, and consequently the absorption efficiency Q_{abs} should be negligible, which is not consistent with the experimental result). From these analyses, we can conclude that the PpIX-encapsulated nanoparticles (average diameter: 25 nm) had a non-negligible scattering efficiency. Furthermore, these nanoparticles showed virtually no extinction in the wavelength region of 700 to 800 nm (which is considered to be an optical window due to the high penetration depth of light in tissue at these wavelengths), but had a strong absorption around 400 nm. This property makes them potentially useful in two-photon excited PDT applications with the light source of a near-infrared laser.[21–23]

The fluorescence emission spectra of the PpIX before and after the encapsulation were almost the same; however, some slight changes of the wavelength and intensity of the fluorescence emission spectra of the PpIX can be observed after the encapsulation. The emission peak of the PpIX after encapsulation was 634 nm, which had red-shifted 2 nm compared with the emission peak of the PpIX before encapsulation; this slight change may be attributed to the surrounding media. Before encapsulation, the PpIX molecules were surrounded by hydrophobic DMSO, while after encapsulation, the PpIX molecules were surrounded by silica nanoparticles dispersed in a hydrophilic aqueous solution.

After encapsulation, the PpIX molecules showed a secondary emission peak around 671 nm, which is also a characteristic emission peak of PpIX.[22] Since the silica nanoparticles could protect the PpIX molecules against direct contact with the aqueous solution and make them more stable chemically, the fluorescence intensity of the PpIX molecules in the 580 to 620-nm and 660 to 700-nm regions became more obvious after encapsulation. Regardless, the fluorescence of PpIX can be easily extracted from the excitation light with a long-wavelength-pass optical filter in fluorescence microscopy.

3.2 *Results of ROS Detection*

The released $^1O_2$ was detected indirectly using DPBF as a $^1O_2$ chemical probe.[18] The DPBF reacted irreversibly with the $^1O_2$ generated by the photoexcitation of the PpIX-encapsulated nanoparticles, and the reaction was easily monitored by recording the decrease (with time) in the absorption intensity of the DPBF at 407 nm. The changes in the absorption spectra of DPBF with time after the irradiation in the presence of nanoparticles were obvious, as shown in Figs. 5(a) and 5(d). The slope of curve "a" in Fig. 5(d) is an indication of the efficiency of generating $^1O_2$ (a steeper slope corresponds to a higher efficiency). To show that the absorption decrease of DPBF was really caused by the $^1O_2$, two control experiments were carried out under the same experimental conditions. As shown in Fig. 5(b) and 5(d), irradiation at 532 nm over 7 minutes caused almost no change in the absorption the PpIX-encapsulated nanoparticles without DPBF probes, which indicated that the absorption property of the PpIX-encapsulated nanoparticles was not affected by the generated $^1O_2$ and light irradiation. As shown in Fig. 5(c) and 5(d), irradiation at 532 nm over 7 minutes caused little change in the absorption of DPBF without the PpIX-encapsulated nanoparticles, which means the DPBF was relatively stable under 532-nm irradiation. These control experiments demonstrate that the decrease in the DPBF absorption at around 407 nm was due only to the simultaneous presence of the PpIX-encapsulated nanoparticles, DPBF, and irradiation, and this $^1O_2$ detection method based on the DPBF probes is effective and convincing.

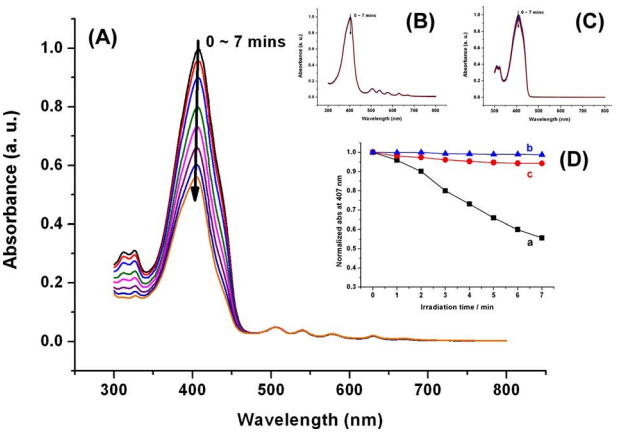

Fig. 5 Absorption spectra at eight different times (measured every minute) of irradiation with a 532-nm laser beam for (A) DPBF in the presence of PpIX-encapsulated nanoparticles; (B) PpIX-encapsulated nanoparticles without DPBF probes; (C) DPBF without PpIX-encapsulated nanoparticles; and (D) normalized decay curves of the absorption density at 407 nm: curve "a" is for DPBF in the presence of PpIX-encapsulated nanoparticles, curve "b" is control #1 for PpIX-encapsulated nanoparticles without DPBF probes, and curve "c" is control #2 for DPBF without nanoparticles. (Color online only.)

3.3 *In Vitro Cell Imaging*

Fluorescence imaging was used to determine whether the PpIX-encapsulated nanoparticles were taken up by the HeLa cells. Figure 6 contains transmission and fluorescence images (under green light excitation) showing that the bright red fluorescence (which was emitted by the PpIX) covered the HeLa cells very well, and the targeting was clear and uniform. No obvious aggregation could be observed (otherwise a large and extremely bright spot would appear). The PpIX molecules were successfully transferred into the HeLa cells using silica nanoparticles as the carriers. Furthermore, the silica nanoparticles were relatively transparent for both the activation light and fluorescence, which helped to maintain the light intensity.

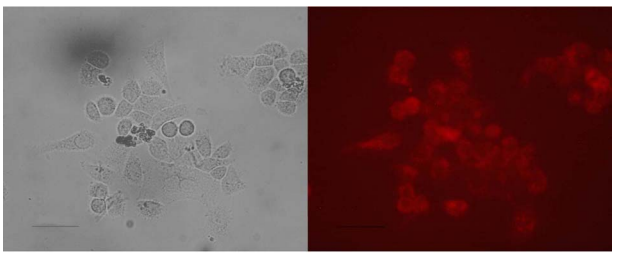

Fig. 6 Fluorescence images of HeLa cells treated with PpIX-encapsulated silica nanoparticles: (a) transmission image of HeLa cells, and (b) the corresponding fluorescence image (scale bar is 50 μm). (Color online only.)

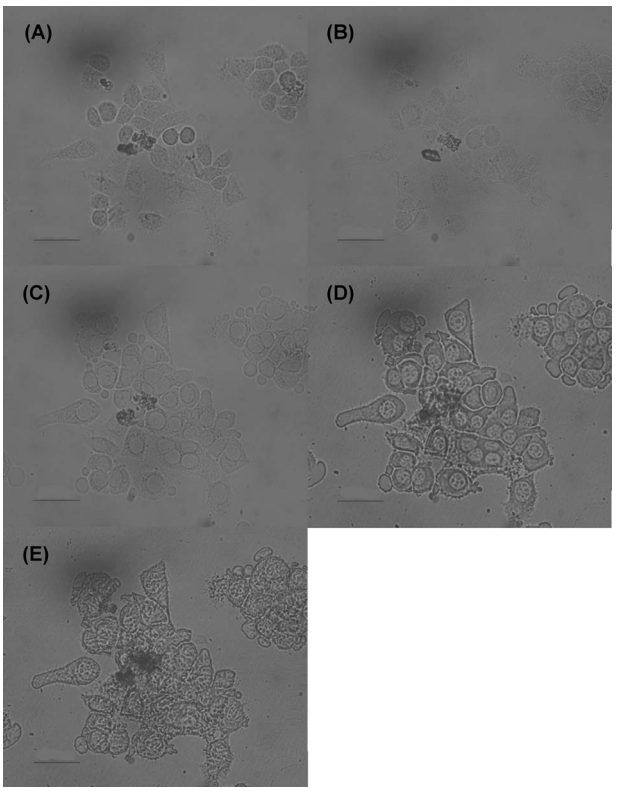

Fig. 7 Transmission images of HeLa cells treated with PpIX-encapsulated silica nanoparticles: (A) before irradiation; (B) after 2-min irradiation; (C) to (E) 2, 4, and 8 min after 2-min irradiation (scale bar is 50 μm).

Herein, the targeting at tumor cells was achieved through the "enhanced permeability and retention" effect (due to the ultrasmall size and surface charge of the PpIX-encapsulated silica nanoparticles). The PpIX-encapsulated silica nanoparticles had net cationic charges on them (Zeta-Potential: +8 mV), and the HeLa cells had anionic charges on their membranes. The favorable electrostatic interaction facilitated the uptake of the cationic amino-functionalized nanoparticles by the HeLa cells. Such targeting can be applied in, e.g., a situation when a tumor site has been localized before the PDT treatment. For an *in vivo* experiment and clinical treatment, certain biomolecules like apo-transferrin and antibodies (whose receptors are over-expressed in cancer cells) can be conjugated with PpIX-encapsulated silica nanoparticles. The biomolecule-conjugated nanoparticles can then accumulate selectively in tumor tissues through receptor-mediated uptake.

3.4 *Results of In Vitro PDT*

The photon-induced toxicity effect of PpIX-encapsulated nanoparticles is shown in Fig. 7. Here we chose a 532-nm light source with a dosage of $\sim$2 mW/cm^2 to treat the HeLa cell plate. After a 2-minute irradiation, the morphology of the HeLa cells did not change much compared with that of the HeLa cells before irradiation. However, 2 minutes after the 2-minute irradiation, the edges of the HeLa cells already showed some morphologic changes that became more and more obvious as time went by. Eight minutes after the irradiation, great changes could be observed in the HeLa cells, and the cell structures were destroyed.

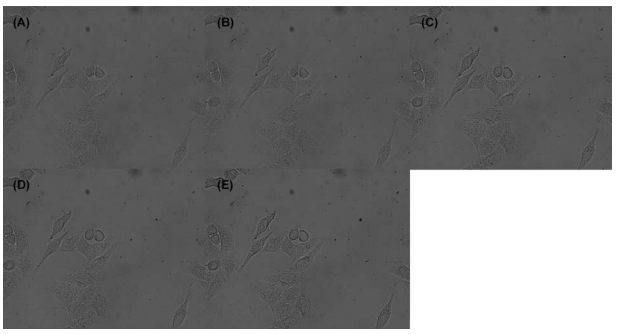

Fig. 8 Transmission images of nontreated HeLa cells: (A) before irradiation; (B) after 2-min irradiation; (C) to (E) 2, 4, and 8 min after 2-min irradiation.

To confirm that the changes in the HeLa cells were related to cell necrosis and were due to the ROS generated by the PpIX, and not due to the toxicity from the light irradiation or silica nanoparticles, the same experimental procedure was carried out for the HeLa cells targeted by Nile red-encapsulated nanoparticles and the nontreated HeLa cells as control experiments. As shown in Fig. 8, no obvious change in the morphology of the nontreated HeLa cells could be observed after the light irradiation, indicating the excitation light power was safe for these cells and did not cause direct toxicity. Figure 9 also shows no obvious change in the morphology of the HeLa cells targeted by Nile red-encapsulated nanoparticles (the fluorescence imaging is also shown in Fig. 9) after the light irradiation, indicating the silica nanoparticles were biocompatible. Here, Nile red is a type of organic fluorescent dye used to track the uptake of silica nanoparticles by fluorescence imaging, not a type of photosensitizer.

By combining the above experimental results, we can conclude that the destruction of the HeLa cells was related to cell necrosis and was induced by the ROSs generated by the PpIX. The whole procedure relied on the fact that oxygen could be well-contacted with encapsulated PpIX, which can be stimulated by light and released. The mesoporosity property of as-

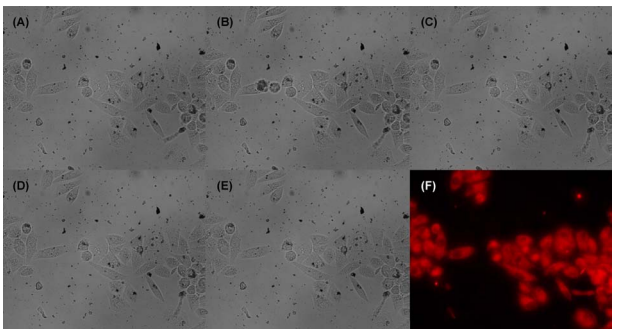

Fig. 9 Transmission images of HeLa cells treated with Nile red-encapsulated silica nanoparticles: (A) before irradiation; (B) after 2-min irradiation; (C) to (E) 2, 4, and 8 min after 2-min irradiation; (F) fluorescence image of HeLa cells treated with Nile red-encapsulated silica nanoparticles. (Color online only.)

synthesized silica nanoparticles is beneficial in all these aspects.

4 Conclusions

In this paper, we described mesoporous silica nanoparticles with encapsulated PpIX used for PDT of cancer. The as-synthesized nanoparticles were of ultrasmall size, highly monodispersed, and stable in an aqueous suspension. These nanoparticles were uptaken by HeLa cells *in vitro*. The photon-induced toxicity effect of PpIX-encapsulated silica nanoparticles was also demonstrated. Colloid mesoporous silica nanoparticles effectively carried the PSs into cancer cells without affecting the function of the activated light and the formation of RDSs. To accumulate PSs selectively in tumor tissues and reduce the dosage of PSs, the surfaces of silica nanoparticles can be functionalized with various groups and further conjugated with proteins[24] or antibodies[25,26] for the specific uptake of cancer cells in future *in vitro* or *in vivo* experiments. PpIX-encapsulated silica nanoparticles can be used as a robust diagnostic and therapeutic tool.

Acknowledgments

This work was partially supported by a multidisciplinary project of Zhejiang University and the Swedish Foundation for Strategic Research (SSF). Jun Qian is grateful to Fuhong Cai for making some theoretical analyses to compare with the experimental results.

References

1. P. N. Prasad, *Introduction to Biophotonics*, Wiley-Interscience, New York (2004).
2. D. E. J. G. J. Dolmans, D. Fukumura, and R. K. Jain, "Photodynamic therapy for cancer," *Nature (London)* **5**, 380–387 (2003).
3. H. I. Pass, "Photodynamic therapy in oncology: mechanisms and clinical use," *J. Natl. Cancer Inst.* **85**, 443–456 (1993).
4. W. M. Star, H. P. Marijnissen, A. E. van den Berg-Blok, J. A. Versteeg, K. A. Franken, and H. S. Reinhold, "Destruction of rat mammary tumor and normal tissue microcirculation by hematoporphyrin derivative photoradiation observed *in vivo* in sandwich observation chambers," *Cancer Res.* **46**, 2532–2540 (1986).
5. I. Wang, N. Bendsoe, C. A. F. Klinteberg, A. M. K. Enejder, S. Andersson-Engels, S. Svanberg, and K. Svanberg, "Photodynamic therapy vs. cryosurgery of basal cell carcinomas: results of a phase III clinical trial," *Brit. J. Dermatol.* **4**, 832–840 (2001).
6. C. A f.Klinteberg, A. M. K. Enejder, I. Wang, S. Svanberg, and K. Svanberg, "Kinetic fluorescence studies of 5-aminolaevulinic acid-induced protoporphyrin IX accumulation in basal cell carcinomas," *J. Photoch. Photobio., B* **49**, 120–128 (1999).
7. Y. N. Konan, R. Gruny, and E. Allemann, "State of the art in the delivery of photosensitizers for photodynamic therapy," *J. Photoch. Photobio., B* **66**, 89–106 (2001).
8. J. Taillefer, M. C. Jones, N. Brasseur, N. J. E. van Lier, and J. C. Leroux, "Preparation and characterization of pH-responsive polymeric micelles for the delivery of photosensitizing anticancer drugs," *J. Pharm. Sci.* **89**, 52–62 (2000).
9. S. Wang, R. Gao, F. Zhou, and M. Selke, "Nanomaterials and singlet oxygen photosensitizers: potential applications in photodynamic therapy," *J. Mater. Chem.* **14**, 487–493 (2004).
10. C. F. van Nostrum, "Polymeric micelles to deliver photosensitizers for photodynamic therapy," *Adv. Drug Delivery Rev.* **56**, 9–16 (2004).
11. Q. Peng, K. Berg, J. Moan, M. Kongshaug, and J. M. Nesland, "5-aminolevulinic acid-based photodynamic therapy: principles and experimental research," *Photochem. Photobiol.* **65**(2), 235–251 (1997).
12. Q. Peng, T. Warloe, K. Berg, J. Moan, M. Kongshaug, K. E. Giercksky, and J. M. Nesland, "5-aminolevulinic acid-based photodynamic therapy-clinical research and future challenges," *Cancer* **79**(12), 2282–2308 (1997).
13. F. J. Arriagada and K. Osseo-Asare, "Synthesis of nanosize silica in aerosol OT reverse microemulsions," *J. Colloid Interface Sci.* **170**, 8–17 (1995).
14. T. K. Jain, I. Roy, T. K. De, and A. N. Maitra, "Nanometer silica particles encapsulating active compounds: A novel ceramic drug carrier," *J. Am. Chem. Soc.* **120**, 11092–11095 (1998).
15. I. Roy, T. Y. Ohulchanskyy, D. J. Bharali, H. E. Pudavar, R. A. Mistretta, N. Kaur, and P. N. Prasad, "Optical tracking of organically modified silica nanoparticles as DNA carriers: A nonviral, nanomedicine approach for gene delivery," *Proc. Natl. Acad. Sci. U.S.A.* **102**, 279–284 (2005).
16. H. Maeda, J. Wu, T. Sawa, Y. Matsumura, and K. Hori, "Tumor vascular permeability and the EPR effect in macromolecular therapeutics. A review," *J. Controlled Release* **65**, 271–284 (2000).
17. J. Choi, A. A. Burns, R. M. Williams, Z. Zhou, A. Flesken-Nikitin, W. R. Zipfel, U. Wiesner, and A. Y. Nikitin, "Core-shell silica nanoparticles as fluorescent labels for nanomedicine," *J. Biomed. Opt.* **12**(6), 064007 (2007).
18. W. Spiller, H. Kliesch, D. Wohrele, S. Hackbarth, B. Roder, and G. J. Schnurpfeil, "Singlet oxygen quantum yields of different photosensitizers in polar solvents and micellar solutions," *J. Porphyr. Phthalocyanines* **2**, 145 (1998).
19. H. C. van de Hulst, *Light Scattering by Small Particles*, Wiley-Interscience, New York (2004).
20. B. N. Khlebtsov, V. A. Khanadeev, and N. G. Khlebtsov, "Determination of the size, concentration, and refractive index of silica nanoparticles from turbidity spectra," *Langmuir* **24**, 8964–8970 (2008).
21. G. S. He, P. P. Markowicz, T. C. Lin, and P. N. Prasad, "Observation of stimulated emission by direct three-photon excitation," *Nature (London)* **415**, 767–770 (2002).
22. S. Lu, J. Chen, Y. Zhang, J. Ma, P. N. Wang, and Q. Peng, "Fluorescence detection of protoporphyrin IX in living cells: a comparative study on single- and twophoton excitation," *J. Biomed. Opt.* **13**(2), 024014 (2008).
23. R. L. Goyan and T. C. David, "Near-infrared two-photon excitation of protoporphyrin IX: Photodynamics and photoproduct generation," *Photochem. Photobiol.* **72**(6), 821–827 (2000).
24. J. Qian, K. T. Yong, I. Roy, T. Y. Ohulchanskyy, E. J. Bergey, H. H. Lee, K. M. Tramposch, S. He, A. Maitra, and P. N. Prasad, "Imaging pancreatic cancer using surface-functionalized quantum dots," *J. Phys. Chem. B* **111**, 6969–6972 (2007).
25. C. Loo, A. Lowery, N. Halas, J. West, and R. Drezek, "Immunotargeted nanoshells for integrated cancer imaging and therapy," *Nano Lett.* **5**(4), 709–711 (2005).
26. X. Huang, I. H. El-Sayed, and M. A. El-Sayed, "Cancer cell imaging and photothermal therapy in the near-infrared region by using gold nanorods," *J. Am. Chem. Soc.* **128** 2115–2120 (2006).